The *Arabidopsis* homologs of trithorax (ATX1) and enhancer of zeste (CLF) establish 'bivalent chromatin marks' at the silent *AGAMOUS* locus

Abdelaty Saleh[1], Ayed Al-Abdallat[1,2], Ivan Ndamukong[1], Raul Alvarez-Venegas[1,3] and Zoya Avramova[1,*]

[1]School of Biological Sciences, UNL, Lincoln, NE 68588, USA, [2]Faculty of Agriculture, University of Jordan, Amman 11942, Jordan and [3]Department of Genetic Engineering, Centro de Investigacion y de Estudios Avanzados-Unidad Irapuato, México

ABSTRACT

Tightly balanced antagonism between the Polycomb group (PcG) and the Trithorax group (TrxG) complexes maintain *Hox* expression patterns in *Drosophila* and murine model systems. Factors belonging to the PcG/TrxG complexes control various processes in plants as well but whether they participate in mechanisms that antagonize, balance or maintain each other's effects at a particular gene locus is unknown. CURLY LEAF (CLF), an *Arabidopsis* homolog of enhancer of zeste (EZ) and the ARABIDOPSIS HOMOLOG OF TRITHORAX (ATX1) control the expression of the flower homeotic gene *AGAMOUS* (*AG*). Disrupted *ATX1* or *CLF* function results in misexpression of *AG*, recognizable phenotypes and loss of H3K4me3 or H3K27me3 histone H3-tail marks, respectively. A novel idea suggested by our results here, is that PcG and TrxG complexes function as a specific pair generating bivalent chromatin marks at the silent *AG* locus. Simultaneous loss of ATX1 and CLF restored *AG* repression and normalized leaf phenotypes. At the molecular level, disrupted *ATX1* and *CLF* functions did not lead to erasure of the CLF- and ATX1-generated epigenetic marks, as expected: instead, in the double mutants, H3K27me3 and H3K4me3 tags were partially restored. We demonstrate that ATX1 and CLF physically interact linking mechanistically the observed effects.

INTRODUCTION

Polycomb group (PcG) complexes maintain the silencing of *Hox* genes, whereas TrxG maintain their expression (1–3). Two major classes of PcG repressor complexes (PRCs) have been recognized in animal systems: PRC2, containing EZ responsible for the histone H3 lysine 27 methylation, and PRC1, mediating the formation of transcription-resistant chromatin structure at target genes (4,5). Complexes containing the Trithorax histone H3 lysine 4-methyl transferase activity are COMPASS, in yeast, and TAC1, in *Drosophila* (6,7). PcG and TrxG factors regulate plant genes as well but plants have developed epigenetic mechanisms that are related, although not identical, with those of animals or yeast (8–11). For example, the PRC2 complex is conserved both structurally and functionally between animals and plants (9,12) but PRC1 homologs have not been identified. *Arabidopsis* components of PcG/TrxG complexes play repressing and activating roles for a number of plant genes (13–21) but whether PcG and TrxG act as antagonists at the same gene locus in plants is unknown. The *Arabidopsis CLF* gene encodes an EZ homolog, while the *ATX1* gene encodes a Trx-homolog, acting as a repressor and activator of the homeotic *AGAMOUS, AG*, gene, respectively. Disruption of either function causes recognizable phenotypes (13,14). Here, we report that nucleosomes at silent *AG* loci carry both the activating, H3K4me3, and the repressing, H3K27me3, marks. Recent findings have suggested that simultaneously present H3K4me3 and H3K27me3 marks establish bivalent chromatin states of silent genes poised for transcription later in life (22). Furthermore, simultaneous loss of both *ATX1* and *CLF* functions caused a remarkable shift towards the wild type. Analyzing the molecular mechanism behind this event we found that, contrary to expectations, loss of both functions resulted in partial restorations of the K4 and K27 marks on the *AG* nucleosomes in the double mutants. The results suggest that the antagonistic PcG- and TrxG-complexes form specific pairs to generate bivalent chromatin marks. The most unexpected result was the partial restoration of the methylation patterns and

*To whom Correspondence should be addressed. Tel: +402 472 3993; Fax: +402 472 2083; Email: zavramova2@unl.edu

phenotypes in the double mutants. It suggested that in the absence of both ATX1 and CLF their roles could be undertaken by a different pair of antagonists. Restored patterns, however, were not identical with the initial patterns, an observation that could account for the variability and instability of phenotypes often seen in epigenetic mutants. Lastly, we demonstrate that ATX1 and CLF physically interact mechanistically linking the observed effects.

MATERIALS AND METHODS

Plant material

Homozygous *atx1*, *clf-1*, $atx1^-/^- clf^-/^-$ and control wild type *Arabidopsis thaliana* (Ws), plants were grown under long day light conditions (14 h light/10 h darkness) at 24°C and similarly handled. *atx1* plants were crossed with *clf-1* both as the female and the male parent with no change of phenotypes or methylation profiles. Homozygocity of $atx1^-/^- clf^-/^-$ lines was verified by PCR, RT-PCR and genetically after backcrossing to single mutant $atx1^-/^-$ and $clf^-/^-$ lines (Supplementary Table 1).

RT-PCR analysis

Total RNA was isolated using Invisorb Spin Plant RNA Mini Kit (Invitek, Berlin, Germany) according to the manufacturer's instruction. First-strand cDNA synthesis was performed on 500 ng of RNA using M-MLV system for RT-PCR (Invitrogen) followed by PCR amplification with Taq DNA Polymerase (Invitrogen) according to the manufacturer's recommendation. PCR primers used for both RT-PCR and ChIP assays are shown in Supplementary Table 2. All PCR amplification reactions were carried out for 38 cycles (95° for 3 min, 95° for 30 min; 50° for 30 min; 72° for 10 min).

ChIP assays were performed following protocols as described (23). Anti-methylated histone antibodies obtained from different sources (Upstate) and (Abcam) were used to confirm reproducibility of patterns. Antibodies specific against ATX1 were raised in rabbits (CoCalico). Band intensities were quantified using ImageQuant™. Intensities were normalized versus the input sample, representing 15% of the DNA used as template (23). Each immunoprecipitation experiment was independently performed, as biological replicates, 3–5 times over a period of several months.

Protein–protein interactions

For testing protein interactions in yeast, ATX1 and CLF (cloned both as bait and pray in the pGBKT7 and pGADT7 vectors, respectively) were tested in the YEASTMAKER Yeast Transformation System' kit (Clontech). Transformed yeast cells were grown on selective, high stringency, SD media lacking leucine, trypotphan, histidine and adenine. Growth was monitored over 15-day period. Growth of serially diluted transformed cells is shown in Supplementary Data (Figure 1). For the BiFC approach, CLF (At2g23380) and ATX1 (At2g31650) genes were amplified from cDNA templates

using specific primers (GATEWAY®, Invitrogen GmbH, Karlsruhe, Germany). The PCR products were subsequently recombined into BiFC vectors (pE-SPYNE, pE-SPYCE) and YFP vector (pENSG-YFP), respectively (24) by attL × attR (LR) recombination at the GATEWAY™ recombination sites. BiFC vectors were kindly provided by C.S. Mayer and W. Dröge-Laser, Georg August University of Goettingen, Germany). The pDONR entry vectors were recombined with the BiFC destination vectors (pE-SPYNE and pE-SPYCE) in an LR reaction which placed the genes in frame with and downstream of the coding sequence of the YFP halves. The resulting expression vector drives expression of the fusion protein under the control of the 35S promoter. The control vectors pE-SPYNE(-)and pE-SPYCE(-) contained the YFP halves with the gateway cassettes replaced by 'inert filler' sequences. The generated ATX-YN/ CLF-YC, ATX-YC/CLF-YN and control ATX-YN/ (-)YC, CLF-YC/(-)NC constructs were delivered into onion epidermal cells and observed 24 h later. Coding sequences of two cytoplasmic proteins (EF1a and MYO1) were cloned in each of the vectors and used as negative controls for the complementation of ATX1.

Transient transformation of onion epidermal cells was carried out using the Helium Biolistic gene transformation system (BioRad, Hercules, CA, USA) tissue using a standard procedure with modifications (25,26). Co-bombardments were carried out with a total of 20 µg of DNA used per shot. Ten microgram of each plasmid was used in the combinations: pE-SPYNE –ATX/ pE-SPYCE-CLF and pE-SPYNE –CLF/pE-SPYCE-ATX. Bombardments were repeated at least three times for each construct. Subcellular localization of fusion proteins was determined by Olympus FV500 Confocal Microscopy using an excitation wavelength of 488 nm. Emission was captured with a 532 nm band pass emission filter.

RESULTS

Loss of both ATX1 and CLF functions rescue single-mutant phenotypes

Derepression of *AG* is partly responsible for the curly phenotype of *Arabidopsis* leaves and for the early flowering of *clf* mutants (14). The rosette leaves of *atx1* mutants are not curled but are smaller and slightly serrated; *atx1* plants also bolt earlier than wild type (Figure 1a and b). After introducing $atx1^-/^-$ in the *clf* background, however, the phenotypes of homozygous double mutant plants shifted towards wild type: leaf-phenotype and flowering time of *atx1/clf* mutants were remarkably different from the single *atx1* and *clf* mutants and phenocopied the wild type (Figure 1a and b); accordingly, *AG* was not detectably expressed in double mutant leaves (Figure 1c).

Rescue of *clf* phenotypes by the loss of ATX1 (and vice versa) implied antagonistic interactions. To determine epistasis, we tested the expression of *ATX1* in the *clf* background and of *CLF* in the *atx1* background. Lack of significant effects (Figure 1c) indicated that ATX1 was not involved in *CLF* expression and CLF did not affect *ATX1*
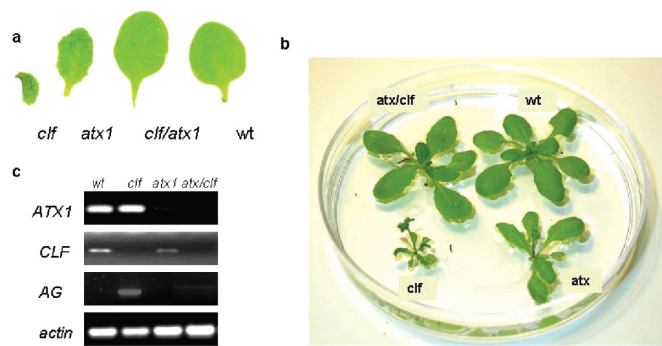
Figure 1. Phenotypes and expression of the homeotic gene *AG* in wild type, in single, and in double mutant plants. (**a**) Fourth rosette leaf from single (*clf* or *atx1*), from double (*atx1/clf*) mutant, and from wild type (wt) plants. (**b**) Same age plants are at different stages of development: *atx1* and *clf* mutants are flowering, while *atx1/clf* and wt plants are still at vegetative stages and (**c**) expression of the *CLF, ATX1* and *AG* genes in the different genetic backgrounds; *ACTIN7*, amplified from the respective templates under the same number of cycles is shown as a loading control. All samples were amplified from the same template.

suggesting that, most likely, *ATX1* and *CLF* do not function in the same genetic pathway.

Methylation patterns of histone H3 lysine 27 and lysine 4 of *AG* nucleosomes at the silent loci

To reveal the molecular mechanism behind these effects, we analyzed the methylated profiles of histone H3 tails of *AG* nucleosomes in young (10-day) seedling and in leaf-chromatins where the *AG* gene is not transcribed (27). ATX1 carries HMT activity trimethylating lysine 4 (H3K4me3) (23), while CLF trimethylates K27/H3 of specific *Arabidopsis* genes (28–31). Immunoprecipitated wild type and *clf* seedling chromatins (with antibodies distinguishing di- and the tri-methylated K27/H3 isoforms) showed loss of H3K27me3 from *AG-clf* nucleo-somes (Figure 2a and b) implicating CLF in trimethylat-ing *AG*-K27/H3. The activity is specific: *SUPERMAN* (*SUP*) and *APETALA1 (AP1)* nucleosomes did not loose their K27/H3 marks in the *clf* background (Figure 2a and b) consistent with reported ability of CLF to regulate *AG* but not *SUP* and *AP* (14,30).

H3K27me3 is the predominant modification of wild type *AG* nucleosomes at both the 5′-transcription start site and at downstream gene (G)-regions (Figure 3a and c). H3K9me2 and H3K27me2 signals were low and did not change significantly in either *atx1* or *clf* backgrounds ($P > 0.05$). Interestingly, nucleosomes from the silent *AG* gene carried also trimethylated K4 (Figure 3a and b). However, H3K4me3 is not sufficient to override the *AG*-non-transcribed state imposed by the presence of H3K27me3. Simultaneously present H3K27me3 and H3K4me3 marks in young seedling chromatin reflect chromatin states, referred to as bivalent, shown recently to silence genes poised for expression later in development (22). Accumulation of H3K4me3 at the *AG*-transcription start site correlates with derepression in the absence of H3K27me3 but with low expression when present together (Figures 1c and 3a), similar to the animal model (22).
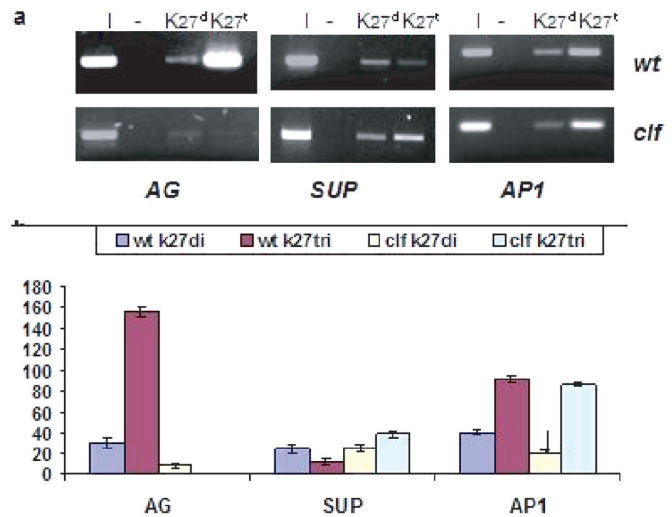
Figure 2. H3K27me2 and H3K27me3 profiles of three Arabidopsis genes. (**a**) ChIP assays with antibodies specific against di- and tri-methylated H3K27; superscripts 't' and 'd' stand for the tri-, or di-methylated isoforms, respectively. (I)-input sample is 15% of the immunoprecipitated DNA; (-) is negative control without antibody. Quantified bands from three independently performed ChIP assays are shown as graphs. Changes in H3K27me3 levels of wild type and *clf SUP* and *AP1* nucleosomes are insignificant ($p > 0.5$).

In contrast to H3K27me3, H3K4me3 is concentrated at the 5′-end *AG*-nucleosomes.

To check for possible presence of ATX1 at the *AG* locus, we performed ChIP assays with ATX1-specific antibodies. The results suggested binding of ATX1 to *AG*-nucleosomes at the transcription start site but absent from downstream (G)-nucleosomes (Figure 4). Thereby, ATX1 and H3K4me3 distribution domains overlap, supporting a role of ATX1 in *AG*-K4-trimethylation. Interestingly, ATX1 was bound to the 5′-end *AG* nucleosomes even when transcription was off. We note also that ATX1 was not bound to *AP1* nucleosomes, despite the ATX1-activation of *AP1* transcription (13). The results suggest that ATX1 controls *AP1* indirectly.

In *clf* chromatin, the H3K27me3 signal disappeared but the H3K4me3 remained. This profile paralleled *AG* derepression, as well as the appearance of the 'curly' phenotype (Figure 3a). Unexpectedly, loss of H3K4me3 in *atx1* chromatin concurred with loss of H3K27me3 implicating ATX1 in the trimethylation of K27. The effects are *AG*-specific: *AP1* sequences were amplified from the same chromatin preparations attesting to the quality of the template (Figure 3d). *ACTIN7*, used as additional control, showed H3K4me3-bands in *atx1* chromatin, indicating that absent K4me3 signals were not due to immunoprecipitation artifacts or poor templates (Figure 3e).

Methylation patterns of histone H3 lysine 27 and lysine 4 in *atx1/clf* double mutants

Functional relevance of ATX1-CLF interaction was pursued further by determining the *AG* methylation patterns in *atx1/clf* double mutants. We predicted that no H3K27me3 or H3K4me3 marks would be present in
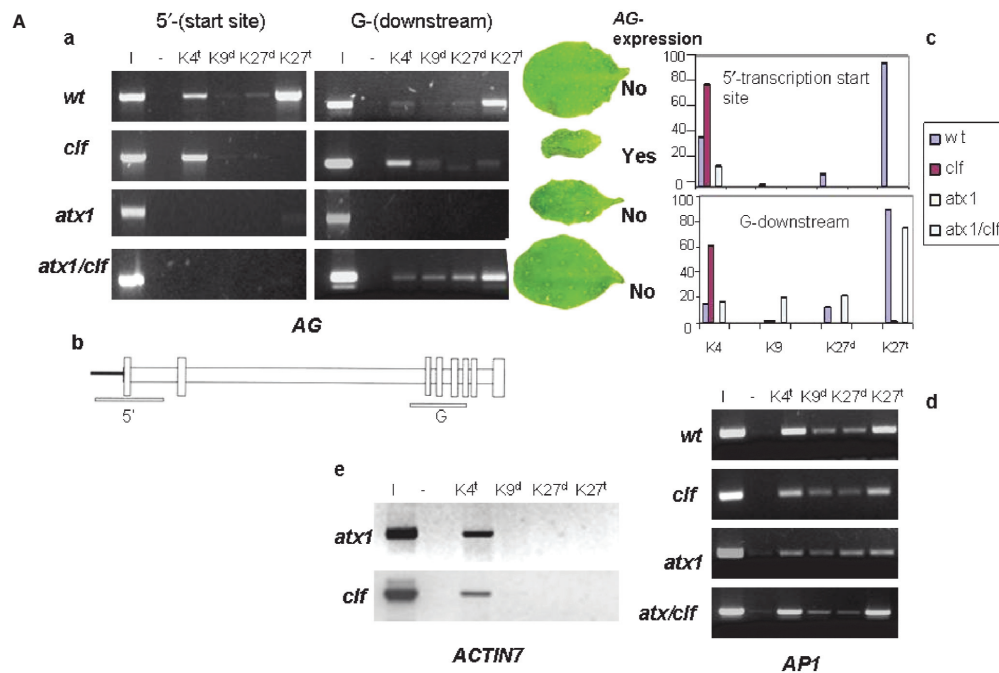
Figure 3. Methylation profiles of histone H3-tail lysines of *AG*-nucleosomes. (**a**) ChIP assays with antibodies specific against tri-methylated H3K4 di- and tri-methylated H3K27, and di-methylated H3K9. Amplified regions are from the 5′-transcription start site and from downstream gene (G)-regions (see **b**). The characteristic leaf phenotypes are shown in parallel with the methylation patterns at 5′-end and downstream nucleosomes, and corresponding expression of *AG* is indicated; (**b**) schematic representation of the *AG* gene: empty vertical boxes represent exons, horizontal boxes represent introns. Bars below the line show regions amplified in the PCR-assay; 5′-represents the region upstream of the transcription start site; G (gene) stands for downstream coding sequences; (**c**) quantified bands showing the relative change in methylation modifications at the 5′-end and the downstream (G)-nucleosomes; results are from three independently performed ChIP assays; (**d**) the *AP1*-methylation profiles are shown as controls illustrating the quality of the templates; the same amounts of template DNA were used in the respective amplification experiments and (**e**) *ACTIN7*, a constitutively expressed gene carries only 'activating' m³K4/H3 tags.

the absence of both ATX1 and CLF. Contrary to the expectation, however, H3K27me3 and H3K4me3, in addition to low levels of H3K9me2 and H3K27me2, were revealed on downstream (G)-nucleosomes but not on 5′-end nucleosomes (Figure 3a). The patterns were reproducible and overall levels of H3K4me3 and H3K27me3 in the *clf/atx1* background were comparable to wild type ($p < 0.3$ for both H3K4me3 and H3K27me3). A notable difference, however, was the presence of H3K4me3 and H3K27me3 tags on downstream-, but not promotor-associated, nucleosomes. Thereby, restored patterns were not identical with the wild type. In support, within homozygous $atx1^-/^-clf^-/^-$ lines 'normalized' phenotypes were displayed by ~95% of the plants. About 5% of progenies of wild-type looking double mutants ($n = 333$; mean value 5.5; SD: 1.36) reverted to smaller, precociously bolting, small rosette-leave (some curled) phenotypes. These results have an important implication for interpreting spontaneous reversals in epigenetic events, as discussed later.

Re-appearance of H3K27me3 and H3K4me3 indicated that HMT activities, different from ATX1 and CLF, could undertake *AG*-modifications but only when both ATX1 and CLF were absent. Restoration of H3K27me3 on (G)-nucleosomes is apparently sufficient to silence *AG* and to rescue phenotypes associated with loss of *CLF* and *ATX1*. The dependence of K27-trimethylation upon
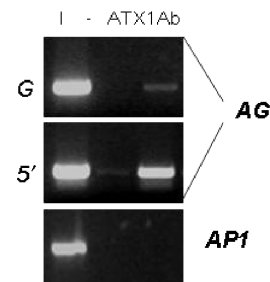

Figure 4. ChIP assays with antiATX1 antibodies. Bands corresponding to the 5′-end *AG*-region amplified after a ChIP with antiATX1 antibodies; downstream region nucleosomes were only weakly represented in the precipitated fraction, while *AP1* nucleosomes were not found in the ATX1-bound fraction.

ATX1 suggests that ATX1 and CLF 'communicate' at *AG*-nucleosomes.

ATX1 and CLF physically interact

To get a clue about the molecular mechanism of the ATX1-CLF communication, we tested their ability to bind each other. In earlier studies, while using ATX1 as bait, we had isolated an ATX1-interacting clone from yeast and have identified it as CLF (unpublished data). At the time, we did not pursue this observation further but the current results prompted us to revisit this finding. Cloned
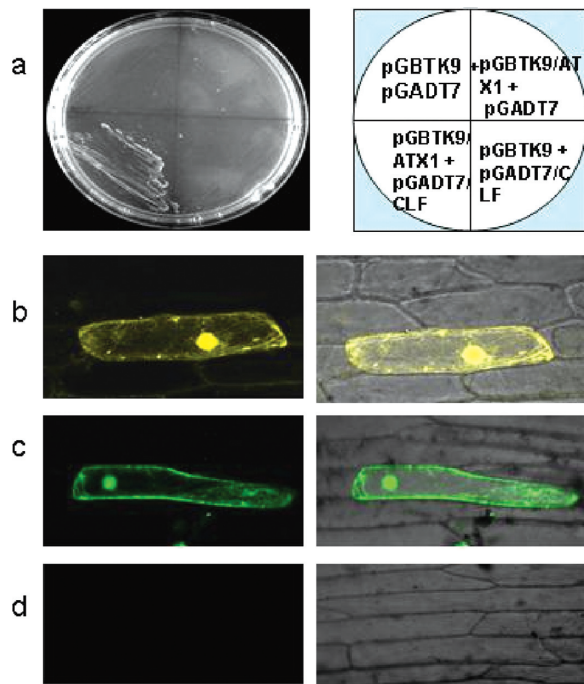
Figure 5. Interaction of ATX1- and CLF-in yeast and in plant cells. (**a**) ATX1 and CLF cloned as bait and prey in the pGBKT9 and the pGADT7 vectors; yeast cells transformed with the constructs, as shown, and grown on selective SD media lacking leucine, tryptophan, histidine and adenine (high stringency); (**b**) BiFC assay of ATX1-YN/CLF-YC. The yellow signal indicates binding of ATX1 and CLF fusion proteins inside the nucleus; (**c**) BiFC assay of ATX1-YC and CLF-YN (ATX1 and CLF expressed in the opposite combinations of YFP-peptides). Fluorescence is shown in green, using a filter, to distinguish interactions of a different combination of complementing YFP-halves. (**d**) Cells transformed with the control vectors ATX1-YN/(-)YC and CLF-YN/(-)YC did not generate fluorescence. The images on the right represent merges of the left images with the DIC images.

reciprocally as 'prey' and 'bait' and tested under two different stringency conditions, CLF and ATX1 did show interaction in yeast (Figure 5a; Supplementary Figure 1). To establish whether ATX1 and CLF would bind in plant cells as well, we used a novel approach developed for the visualization of interactions between proteins in living cells: non-fluorescent fragments of YFP could reconstitute the fluorophore only when brought together by interactions between proteins covalently linked to each fragment (32). ATX1 and CLF were cloned as fusion proteins with halves of the YFP protein and transiently expressed in plant cells to be inspected by the bimolecular fluorescence complementation (BiFC) approach. Accordingly, the fluorescence seen in the nuclei of transformed onion epidermal cells (Figure 5b and c) demonstrate that ATX1 and CLF physically interact. Vectors expressing the YFP halves alone did not produce any signal; nor did the EF1α protein, cloned and tested as a complementary half for the ATX1-linked fluorophore. These experiments underscored the specificity of the ATX1-CLF interaction (Figure 5d). Moreover, loss of H3K27me3 in the *atx1* background implicated ATX1 in recruiting CLF to *AG*-nucleosomes. Attempts to co-immunoprecipitate recombinantly produced in *Escherichia coli* ATX1 and CLF were

unsuccessful suggesting that protein modifications might be involved and required in their interaction.

DISCUSSION

Our findings offer novel insights into the workings of the *Arabidopsis* PcG and TrxG antagonists. An interaction between ATX1 and CLF for the control of the *AG* silent state is supported by three types of evidence: first, restoration of *AG*-repression in the double mutants and rescued leaf phenotypes associated with *AG* misexpression in single *atx1* and *clf* mutants, provide compelling genetic evidence; second, bivalent chromatin marks established by the two methylases at the silent *AG* locus constitute epigenetic evidence. Lastly, the propensity of ATX1 and CLF to form specific complexes *in vivo* mechanistically links the observed effects. Restoration of *AG* repression upon loss of both ATX1 and CLF and loss of H3K27me3 in the *atx1* background support the idea that the two methylases interact. Partial restoration of the H3K4me3 and H3K27me3 signals in the double *atx1/clf* mutants illustrated that *AG*-nucleosomes could be targeted by a different (surrogate) pair of methylases but only when both ATX1 and CLF were absent. Why methylations were restored on downstream nucleosomes but not at the 5′-nucleosomes is unclear but one plausible possibility is that a specific transcription factor directing ATX1 and CLF to the promotor does not interact with the surrogate pair.

Presence of both K4me3 and K27me3 tags at silent embryonic stem cell loci was interpreted as a bivalent mark on genes poised for transcription later in development (22). It is quite remarkable, then, that a similar bivalent mark was found at the flower homeotic gene, silent in young seedlings but expressed during flowering (33). ChIP assay, currently used for determining chromatin modification states, is not a feasible approach for analysis of the active *AG* profiles because flower chromatin is a mix of cells (whorls) expressing and non-expressing *AG* (33). Alternative approaches need to be developed to assess *AG* modification patterns in flowers.

It is interesting to note that the nucleosomes of another homeotic regulator, *AP1*, also carry the bivalent K4me3 and K27me3 marks in silent chromatins (Figures 2a and 3d). However, an apparently different antagonistic pair establishes the bivalent marks of *AP1* nucleosomes because the K27me3 signal in *clf* chromatin is preserved as is the K4me3 signal in *atx1* chromatin (Figures 1d and 2c). While CLF does not affect *AP1* (14), consistent with preservation of K27me3 in *clf* chromatin, ATX1 activates *AP1* transcription (13). ChIP analysis with antiATX1 antibodies did not reveal presence of ATX1 at *AP1*nucleosomes (Figure 4) consistent with a conclusion that ATX1 does not modify *AP1* nucleosomes. Thereby, activation of *AP1* transcription is, most likely, indirect.

De-repression of *AG* in *clf* mutants is associated with a strong curly leaf phenotype (14) but, interestingly, *atx1* plants also show a leaf phenotype despite the fact that *AG* is not expressed in *atx1* leaf chromatin (Figure 1a and c). Most likely, other ATX1-regulated genes contribute to

leaf size and shape; in addition, both H3K4me3 and H3K27me3-tags might be needed to establish 'normal' silencing of *AG*. We note also that the *AG* transcription pattern as well as histone H3-K4, K9 and K27 methylation profiles of *AG*-nucleosomes did not depend on the genetic background of the plants as they were indistinguishable in chromatins isolated from Col, Ws and Ler background plants. Furthermore, the bivalent-state silencing 'code' may be gene-specific; for instance, Clarke Kent epialleles of *SUP* require simultaneously present H3K27me2 and H3K9me2 to maintain DNA methylation and to keep the gene silent (31).

There are three *EZ* and multiple *ATX1*-related and putative K4-trimethylase genes in the genome of *Arabidopsis* (16,34,35). At least three different PRC2-like complexes, containing different EZ homologs, have been proposed (9,29). Despite some partial redundancy, however, none of the CLF homologs (MEA or SWN) could complement *clf* mutants consistent with the idea that each one participates in a different complex (9,14). Likewise, the inability of any of the ATX1-related proteins to substitute for ATX1 in the *atx1* background (Figure 1a and b; 14,23) suggest that K4 methyl transferases assemble, most likely, distinct complexes as well. Given that a functionally equivalent methylase cannot substitute a missing relative within a complex, our results take the specificity one step further, by suggesting that PcG- and TrxG-complexes form specific pairs establishing bivalent marks at targeted loci.

The idea of how two antagonistic epigenetic complexes might interact is illustrated in the proposed model (Figure 6). A central assumption is that each PRC2 and TrxG complex assembles a specific set of subunits around a particular EZ or TRX homolog. Only when both complexes are missing could their roles be undertaken by another pair. Such a model could explain partial rescue of single mutant *atx1* and *clf* phenotypes in the absence of both ATX1 and CLF. Furthermore, restored patterns were not identical with the wild type, i.e. they did not occur at 5'-end nucleosomes, nor did they take place 100% of the times. Thereby, inability of surrogate complexes to fully rescue native patterns provides a basis for interpreting spontaneous reversals, variability and instability of phenotypes associated with epigenetic mutations.

Partial normalization of axial–skeletal transformations in mice, observed when both *Mll* (a human homolog of trithorax) and *BMI*-1 (a PcG component) were deleted, led to the suggestion that direct interaction between MLL and a PcG-subunit was the molecular mechanism of phenotype rescue (36). Here, we demonstrated that the Trx and EZ homologs could, indeed, bind directly; interactions among other subunits of the complex pair are not excluded. It is interesting to consider our results in the context of two recent models of PcG-TrxG interactions in animal systems. At the *UBX*-PRC sites, the Trx protein is constitutively bound with PcG complexes compatible with a possibility that the two complexes might directly interact, although binding partners were not identified (37). It was suggested that Ash1 and Trx HMTases were not 'coactivators' for the activation of *HOX* genes but function as antirepressors of
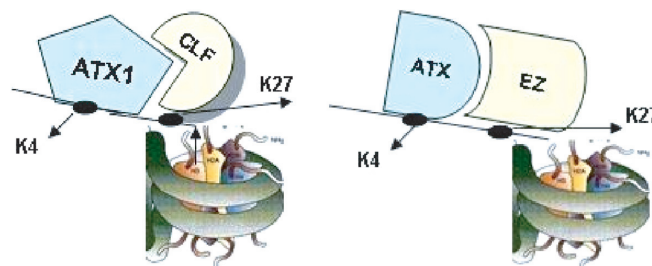
Figure 6. A model for the interaction of the ATX1-containing TrxG and CLF-containing PcG complexes at the *AG* locus. In wild type leaf chromatin, CLF and ATX1 counterbalance each other. At the molecular level, this is associated with non-transcribed *AG* and with presence of m³K4/H3 and m³K27/H3. Both ATX1 and CLF activities are required for the 'normal' repression of *AG* generating, a bivalent chromatin state. ATX1 and CLF participate in antagonistic complexes functioning as a specific pair (nucleosome on the left). Loss of either CLF or ATX1 cannot be substituted by a homologous activity within the pair. ATX1 at the *AG*- 5'-nucleosomes may recruit CLF but not vice versa. This may account for the m³K4 and m³K27 patterns in the single mutants (see text). Elimination of both ATX1 and CLF allows a different pair of antagonists to label *AG* (nucleosome on the right). However, they modify only downstream nucleosomes because the specific factor taking ATX1/CLF to the start site fails to recruit their homologs. Assembly of substitute complexes restoring the methylation tags might not be occurring 100% of the time accounting for the variability in rescued phenotypes.

PcG function to prevent inappropriate silencing of *HOX*. Methylated K4/H3 was suggested to prevent binding of PcG (35). Tri-methylated K4 were confined to the first 1 kb, and tri-methylated K27 were found throughout the coding sequence (38) similar to the H3K27me3 and H3K4me3 distribution at the *AG* locus. However, the molecular mechanism keeping the homeotic *AG* gene silent is apparently different: presence of K4-methylation did not prevent binding of a CLF-containing repressive complex; to the contrary, ATX1 was required for methylations at K27 to occur. Our results agree well with the model suggesting that simultaneous presence of TRX and PcG (and the activating K4 and repressing K27 marks, respectively) establish bivalent chromatin states in embryonic stem cells (22). In a bivalent state, certain genes are silent but the chromatin structure is poised for activation later in development. It is tempting to suggest that the presence of K4- and K27-trimethyl marks at the non-expressing *AG* locus in young seedling chromatin reflects a bivalent chromatin state prepared for expression at a later developmental stage.

SUPPLEMENTARY DATA

Supplementary Data are available at NAR Online.

ACKNOWLEDGEMENTS

REFERENCES

1. Grimaud,C., Negre,N. and Cavalli,G. (2006) From genetics to epigenetics: the tale of Polycomb group and trithorax group genes. *Chromosome Res.*, **14**, 363–375.
2. Hanson,R.D., Hess,J.L., Yu,B.D., Ernst,P., van Lohuizen,M., Berns,A., van der Lugt,N.M., Shashikant,C.S., Ruddle,F.H. *et al.* (1999) Mammalian Trithorax and Polycomb-group homologues are antagonistic regulators of homeotic development. *Proc. Natl Acad. Sci. USA*, **96**, 14372–14377.
3. Ringrose,L. and Paro,R. (2004) Epigenetic regulation of cellular memory by the Polycomb group and thrithorax group proteins. *Annu. Rev. Genet.*, **38**, 413–443.
4. Francis,N.J., Kingston,R.E. and Woodcock,C.L. (2004) Chromatin compaction by a Polycomb group protein. *Science*, **306**, 1574–1577.
5. Levine,S.S., King,I.F.G. and Kingston,R.E. (2004) Division of labor in Polycomb group repression. *Trends Biochem. Sci.*, **29**, 478–485.
6. Miller,T., Krogan,N.J., Dover,J., Erdjument-Bromage,H., Tempst,P., Johnston,M., Greenblatt,J.F. and Shilatifard,A. (2001) COMPASS: a complex of proteins associated with a trithorax-related SET domain protein. *Proc. Natl Acad. Sci. USA*, **98**, 12902–12907.
7. Petruk,S., Sedkov,Y., Smith,S., Tillib,S., Kraevski,V., Nakamura,T., Canaani,E., Croce,C.M. and Mazo,A. (2001) Trithorax and dCBP acting in a complex to maintain expression of a homeotic gene. *Science*, **294**, 1331–1334.
8. Avramova,Z. (2002) Heterochromatin in animals and plants; similarities and differences. *Plant Phys.*, **129**, 40–49.
9. Chanvivattana,Y., Bishopp,A., Schubert,D., Stock,C., Moon,Y.H., Sung,Z.R. and Goodrich,J. (2004) Interaction of Polycomb-group proteins controlling flowering in Arabidopsis. *Development*, **131**, 5263–5276.
10. Loidl,P. (2004) A plant dialect of the histone language. *Trends Plant Sci.*, **9**, 84–90.
11. Meyerowitz,E.M. (2002) Plants compared to animals: the broadest comparative study of development. *Science*, **295**, 1482–1485.
12. Schubert,D., Clarenz,O. and Goodrich,J. (2005) Epigenetic control of plant development by Polycomb-group proteins. *Curr. Opin. Plant. Biol.*, **8**, 553–561.
13. Alvarez-Venegas,R., Pien,S., Sadder,M., Witmer,X., Grossniklaus,U. and Avramova,Z. (2003) *ATX1*, an *Arabidopsis* homolog of *Trithorax* has histone methylase activity and activates flower homeotic genes. *Curr. Biol.*, **13**, 627–634.
14. Goodrich,J., Puangsomlee,P., Martin,M., Long,D., Meyerowitz,E. and Coupland,G. (1997) A Polycomb-group gene regulates homeotic gene expression in *Arabidopsis*. *Nature*, **386**, 44–51.
15. Katz,A., Oliva,M., Mosquna,A., Hakim,O. and Ohad,N. (2004) FIE and CURLY LEAF polycomb proteins interact in the regulation of homeobox gene expression during sporophyte development. *Plant J.*, **37**, 707–719.
16. Kim,S.Y., He,Y., Jacob,Y., Noh,Y.S., Michaels,S. and Amasino,R. (2005) Establishment of the vernalization-responsive. Winter-annual habitat in Arabidopsis requires a putative histone H3 methyl transferase. *Plant Cell*, **17**, 3301–3310.
17. Kohler,C., Hennig,L., Bouveret,R., Gheyselinck,J., Grossniklaus,U. and Gruissem,W. (2003) Arabidopsis MSI1 is a component of the MEA/FIE Polycomb group complex and required for seed development. *EMBO J.*, **22**, 4804–4814.
18. Sung,S. and Amasino,R.M. (2004) Vernalization in Arabidopsis thaliana is mediated by the PHD finger protein VIN3. *Nature*, **427**, 159–164.
19. Sung,S., He,Y., Eshoo,T.W., Tamada,Y., Johnson,L., Nakahigashi,K., Goto,K., Jacobsen,S.E. and Amasino,R.M. (2006) Epigenetic maintenance of the vernalized state in Arabidopsis thaliana requires LIKE HETEROCHROMATIN PROTEIN 1. *Nat. Genet.*, **38**, 706–710.
20. Wood,C.C., Robertson,M., Tanner,G., Peacock,W.J., Dennis,E.S. and Helliwell,C.A. (2006) The Arabidopsis thaliana vernalization response requires a polycomb-like protein complex that also includes VERNALIZATION INSENSITIVE 3. *Proc. Natl Acad. Sci. USA*, **103**, 14631–14636.
21. Yoshida,N., Yanai,Y., Chen,L., Kato,Y., Hiratsuka,J., Miwa,T., Sung,Z.R. and Takahashi,S. (2001) EMBRYONIC FLOWER2, a novel Polycomb group protein homolog, mediates shoot development and flowering in Arabidopsis. *Plant Cell*, **13**, 2471–2481.
22. Bernstein,B.E., Mikkelsen,T.S., Xie,X., Kamal,M., Huebert,D.J., Cuff,J., Fry,B., Meissner,A. and Wernig,M. (2006) A bivalent chromatin structure marks key developmental genes in embryonic stem cells. *Cell*, **125**, 315–326.
23. Alvarez-Venegas,R. and Avramova,Z. (2005) Methylation patterns of histone H3 Lys 4, Lys 9 and Lys 27 in transcriptionally active and inactive *Arabidopsis* genes and in *atx1* mutants. *Nucleic Acids Res.*, **33**, 5199–5206.
24. Weltmeier,F., Ehlert,A., Mayer,C., Dietrich,K., Wang,X., Schutze,K., Alonso,R., Harter,K., Vicente-Carbajosa,J. *et al.* (2006) Combinatorial control of *Arabidopsis* proline dehydrogenase transcription by specific heterodimerisation of bZIP transcription factors. *EMBO J.*, **25**, 3133–3143.
25. Gordon-Kamm,W., Spencer,T., Mangano,M., Adams,T., Daines,R., Start,W., O'Brien,J., Chambers,S., Adams,W.Jr, *et al.* (1990) Transformation of maize cells and regeneration of fertile transgenic plants. *Plant Cell*, **2**, 603–618.
26. Saleh,A., Lumbreras,V., Lopez,C., Puigjaner,E., Kizis,D. and Pagès,M. (2006) Maize DBF1-interactor protein 1 containing an R3H domain is a potential regulator of DBF1 activity in stress responses. *Plant J.*, **46**, 747–757.
27. Sieburth,L.E. and Meyerowitz,E.M. (1997) Molecular dissection of the AGAMUS control region shows that cis elements for spatial regulation are located intragenically. *Plant Cell*, **9**, 355–365.
28. Schonrock,N., Bouveret,R., Leroy,O., Borghi,L., Kohler,C., Gruissem,W. and Hennig,L. (2006) Polycomb-group proteins repress floral activator AGL19 in the FLC-independent vernalization pathway. *Genes Dev.*, **20**, 1667–1678.
29. Makarevich,G., Leroy,O., Akinci,U., Schubert,D., Clarenz,O., Goodrich,J., Grossniklaus,U. and Kohler,C. (2006) Different Polycomb group complexes regulate common target genes in *Arabidopsis*. *EMBO Rep.*, **7**, 947–952.
30. Schubert,D., Primavesi,L., Bishopp,A., Roberts,G., Doonan,J., Jenuwein,T. and Goodrich,J. (2006) Silencing by plant Polycomb-group genes requires dispersed trimethylation of histone H3 at lysine 27. *EMBO J.*
31. Lindroth,A.M., Shultis,D., Jasencakova,Z., Fuchs,J., Johnson,L., Schubert,D., Patnaik,D., Pradhan,S., Goodrich,J. *et al.* (2004) Dual histone H3 methylation marks at lysines 9 and 27 required for interaction with *CHROMOMETHYLASE3*. *EMBO J.*, **23**, 4146–4155.
32. Hu,C.-D., Chinenov,Y. and Kerppola,T.K. (2002) Visualization of interactions among bZIP and rel family proteins in living cells using bimolecular fluorescence complementation. *Mol Cell*, **9**, 789–798.
33. Coen,E.S. and Meyerowitz,E.M. (1991) The war of whorls: genetic interactions controlling flower development. *Nature*, **353**, 31–37.
34. Alvarez-Venegas,R. and Avramova,Z. (2002) SET-domain proteins of the Su(var)3-9, E(z) and trithorax families. *Gene*, **285**, 25–37.
35. Baumbusch,L.O., Thorstensen,T., Krauss,V., Fischer,A., Naumann,K., Assalkhou,R., Schulz,I., Reuter,G. and Aalen,R.B. (2001) The Arabidopsis thaliana genome contains at least 29 active genes encoding SET domain proteins that can be assigned to four evolutionarily conserved classes. *Nucleic Acids Res.*, **29**, 4319–4333.
36. Xia,Z.-B., Anderson,M., Diaz,M.O. and Zeleznik-Le,N. (2003) MLL repression domain interacts with histone deacetylases, the polycomb group proteins HPC2 and BMI-1, and the co-repressor C-terminal-binding protein. *Proc. Natl Acad. Sci. USA*, **100**, 8342–8347.
37. Klymenko,T. and Muller,J. (2004) The histone methyltransferases Trithorax and Ash1 prevent transcriptional silencing by Polycomb group proteins. *EMBO Rep.*, **5**, 373–377.
38. Papp,B. and Mueller,J. (2006) Histone trimethylation and the maintenance of transcriptional ON and OFF states by trxG and PcG proteins. *Genes Dev.*, **20**, 2041–2054.